Preprints, 12th IFAC Workshop on Time Delay Systems
June 28-30, 2015. Ann Arbor, MI, USA

Semi-discretization and the time-delayed PDA feedback control of human balance

Tamas Insperger * **John Milton** ** **Gabor Stepan** *

* *Department of Applied Mechanics, Budapest University of Technology and Economics, Budapest, Hungary (e-mail: insperger@mm.bme.hu, stepan@mm.bme.hu).*
** *The Claremont Colleges, Claremont, CA, USA (e-mail: JMilton@kecksci.claremont.edu).*

Abstract: An important question for human balance control concerns how the differential equations for the neural control of balance should be formulated. In this paper, we consider a discrete-time and a continuous-time delayed proportional-derivative-acceleration controller and establish the transition between them by means of the semi-discretization. We show that the critical delay, which limits stabilizability of the system, is about the same for the continuous-time systems and its semi-discrete counterparts.

Keywords: balancing, reflex delay, acceleration feedback, stability, sampling effect, semi-discretization.

1. INTRODUCTION

Stabilization of unstable equilibria and orbits is a highly important task in engineering and science. Many engineering structures are operated around an unstable position or around an unstable path by means of feedback control. Examples include the control of airplanes, satellites, missiles, trains, brake systems, etc. One reason for the thorough study of balancing tasks is that it is more efficient to perform sudden quick movements from an unstable position than from a stable one. Another beneficial feature is that the energy demand of the control process is relatively small. For the same reasons, living creatures also often stand at or move about unstable positions, since the ability to start quick motions is a vital action in the wildlife. Swimming of fishes, flying of birds or human gait can be mentioned as examples.

As recognized in the 1940s with the development of control theory, time delay typically arises in feedback control systems due to the finite speed of information transmission and data processing. These systems can be described by delay-differential equations (DDEs) and are associated with an infinite-dimensional state space (Michiels and Niculescu, 2007). Human balancing is an important implementation of delayed feedback control. Falls are leading causes of accidental death and morbidity in the elderly. Thus there is a strong motivation to understand the nature of the mechanisms that maintain human balance, why these mechanisms fail and how risks for falling can be minimized. Human balancing processes make typically use of visual, vestibular and mechanoreceptor feedbacks, which are often associated with a proportional-derivative-acceleration (PDA) feedback (Lockhart and Ting, 2007; Welch and Ting, 2008; Insperger et al., 2013). Specifically, the role of acceleration feedback in human balance control have been recently recognized (Peterka et al., 2006; Nataraj et al., 2012).

A fundamentally important question for human balance control which up to now has received little attention concerns how the differential equations for the neural control of balance should be formulated. To illustrate the problem consider a controlled inverted pendulum subjected to a delayed proportional-derivative (PD) controller whose small movements are described by the DDE

$$\ddot{\theta}(t) - \omega_{\mathrm{n}}^2 \theta(t) = -f(t) \tag{1}$$

where θ is the vertical displacement angle, ω_{n} is the natural angular frequency of small oscillations when the pendulum hangs downwards and $f(t)$ describes the control action. Since the left-hand side of (1) describes the motion of a Newtonian dynamical system, it evolves in continuous time. However, since the right-hand side describes a neuro-physiological system it has a distinctly digital quality reflecting, for example, the observation that spatially separated neurons communicate by discrete action potentials. Traditionally mathematical models for stick balancing (Foo et al., 2000; Jirsa et al., 2000; Milton et al., 2009a; Stepan, 2009) have assumed that the feedback is a continuous and smooth function of time. However, a number of experimental observations on human balance and movement suggest that the feedback exhibits a number of properties expected for digital control including the intermittent character of corrective movements (Burdet and Milner, 1998; Cabrera and Milton, 2002; Cluff and Balasubramaniam, 2009; Miall et al., 1993) and the role of central refractory times (van de Kamp et al., 2013). Indeed, for certain balancing tasks, intermittent control works better than continuous control (Insperger et al., 2010; Loram et al., 2011). These observations have prompted many investigators to develop mathematical models which emphasize a role for event- and clock-driven intermittent control strategies (Asai et al., 2009; Cabrera and Milton, 2002; Gawthrop et al., 2013; Insperger and Milton, 2014; Loram et al., 2014). Here we consider the possibility that the neural feedback lies somewhere between these two extremes.

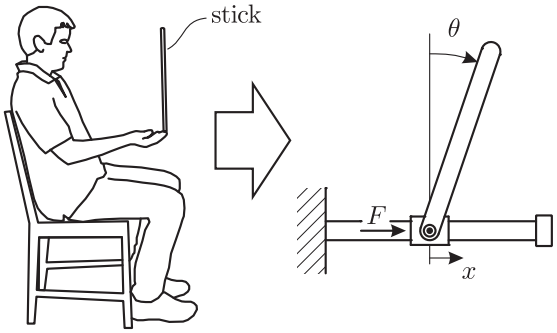

Fig. 1. Mechanical model for stick balancing at the fingertip as a pendulum-cart model.

Namely, we consider a continuous-time and a discrete-time delayed PDA controller and establish the transition between them by means of the semi-discretization. We show that the critical delay, which limits stabilizability of the system, is about the same for the continuous-time systems and its semi-discrete counterpart.

2. MECHANICAL MODEL FOR STICK BALANCING

One of the most studied experimental paradigms for human balance control is stick balancing at the fingertip Cabrera and Milton (2002); Cluff and Balasubramaniam (2009); Lee et al. (2012); Milton et al. (2009b). The corresponding mechanical model is shown in Figure 1. Balance is maintained by the control force $F(t)$, which is determined by a feedback mechanism through the neural system. A simple linear model for this balancing task can be given by (1). If the length and the mass of the pendulum are L and m and the mass of the cart is negligible then $\omega_{\rm n} = \sqrt{6g/L}$ and $f(t) = 6F(t)/(mL)$.

In the context of balance control, PDA feedback arises because the visual, vestibular and proprioceptive sensory systems are able to measure position, velocity and acceleration (Lockhart and Ting, 2007; Welch and Ting, 2008). With respect to the timing of the control actions, two types are analyzed:

- a discrete-time controller without feedback delay; and
- a continuous-time controller with feedback delay.

The transition between these two concepts are established by means of the semi-discretization method (Insperger and Stepan, 2011).

2.1 Discrete-time controller without feedback delay

Discrete-time controller updates the control force at distinct time instants. If the sampling period of the control system is denoted by Δt, then the governing equation reads

$$\ddot\theta(t) - \omega_{\rm n}^2\theta(t) = -k_{\rm p}\theta(t_i) - k_{\rm d}\dot\theta(t_i) - k_{\rm a}\ddot\theta(t_i), \quad t \in [t_i, t_{i+1}), \tag{2}$$

where $t_i = i\Delta t$ are the sampling instants. Here, the control force is kept piecewise constant over each sampling period $[t_i, t_{i+1})$. This phenomenon is called zero-order hold in control theory. Equation (2) can also be written as

$$\ddot\theta(t) - \omega_{\rm n}^2\theta(t) = -k_{\rm p}\theta(t-\rho(t)) - k_{\rm d}\dot\theta(t-\rho(t)) - k_{\rm a}\ddot\theta(t-\rho(t)), \tag{3}$$

where

$$\rho(t) = t - {\rm Int}(t/\Delta t) \tag{4}$$

is a time-periodic delay and Int denotes the integer part function. In other words, for $t \in [t_j, t_{j+1})$, $\theta(t_j - r\Delta t) = \theta(t-\rho(t))$. The graph of the time delay variation is shown in panel a) of Figure 2. Although there is no explicit delay in the feedback mechanism, the zero-order hold still results in a piecewise linear, sawtooth-like time-varying delay. The average delay is

$$\tilde\tau = \frac{1}{\Delta t}\int_0^{\Delta t} \rho(t){\rm d}t = \frac{1}{2}\Delta t. \tag{5}$$

Note that the acceleration is piecewise constant due to the piecewise constant control force. Two types of acceleration feedback are possible:

- the feedback of $\ddot\theta(t_i^-) = \lim_{\varepsilon\to 0}\ddot\theta(t_i - \varepsilon)$, or
- the feedback of $\ddot\theta(t_i^+) = \lim_{\varepsilon\to 0}\ddot\theta(t_i + \varepsilon)$.

Here, we consider the first case, i.e., from now on we use the notation $\ddot\theta(t_i) = \ddot\theta(t_i^-)$.

2.2 Continuous-time controller with feedback delay

The governing equation for the continuous-time delayed PDA controller reads

$$\ddot\theta(t) - \omega_{\rm n}^2\theta(t) = -k_{\rm p}\theta(t-\tau) - k_{\rm d}\dot\theta(t-\tau) - k_{\rm a}\ddot\theta(t-\tau), \tag{6}$$

where $k_{\rm p}$, $k_{\rm d}$, $k_{\rm a}$ are the proportional, derivative and acceleration control gains, and τ is the feedback delay. Here, the control force is continuously updated based on the delayed position, velocity and acceleration. Still, the control force is typically discontinuous in time, since initial discontinuities of the acceleration are transmitted to the control force. (Note that (6) is a neutral functional differential equation, thus the initial discontinuities do not decay in time as opposed to retarded functional differential equation.)

2.3 Semi-discretization of time-delayed feedback

A transition between the continuous-time and the discrete-time controllers can be established by means of the semi-discretization method (Insperger and Stepan, 2011). The semi-discretized equation which corresponds to (6) is

$$\ddot\theta(t) - \omega_{\rm n}^2\theta(t) = -k_{\rm p}\theta(t_{i-r}) - k_{\rm d}\dot\theta(t_{i-r}) - k_{\rm a}\ddot\theta(t_{i-r}), \quad t \in [t_i, t_{i+1}), \tag{7}$$

where the $r \in \mathbb{Z}$ is an integer called discrete delay. The control force is determined using discrete delayed values of the angular position, angular velocity and angular acceleration and is kept piecewise constant over each sampling period $[t_i, t_{i+1})$. In this model therefore both a feedback delay of magnitude $r\Delta t$ and a zero-order hold appears. This system can also be written in the form of equation (3), but the time-varying delay now reads

$$\rho(t) = r\Delta t + t - {\rm Int}(t/\Delta t) \tag{8}$$

instead of (4). The graph of the time delay variation for $r = 1$ and for $r = 2$ is shown in panels b) and c) of Figure 2. The average delay is

$$\tilde\tau = \frac{1}{\Delta t}\int_0^{\Delta t} \rho(t){\rm d}t = \left(r + \frac{1}{2}\right)\Delta t. \tag{9}$$

Let us fix the average delay $\tilde\tau$ to be equal to the delay τ in 6). Then transition between equations (2) and (6) can be established by increasing the discrete delay r and

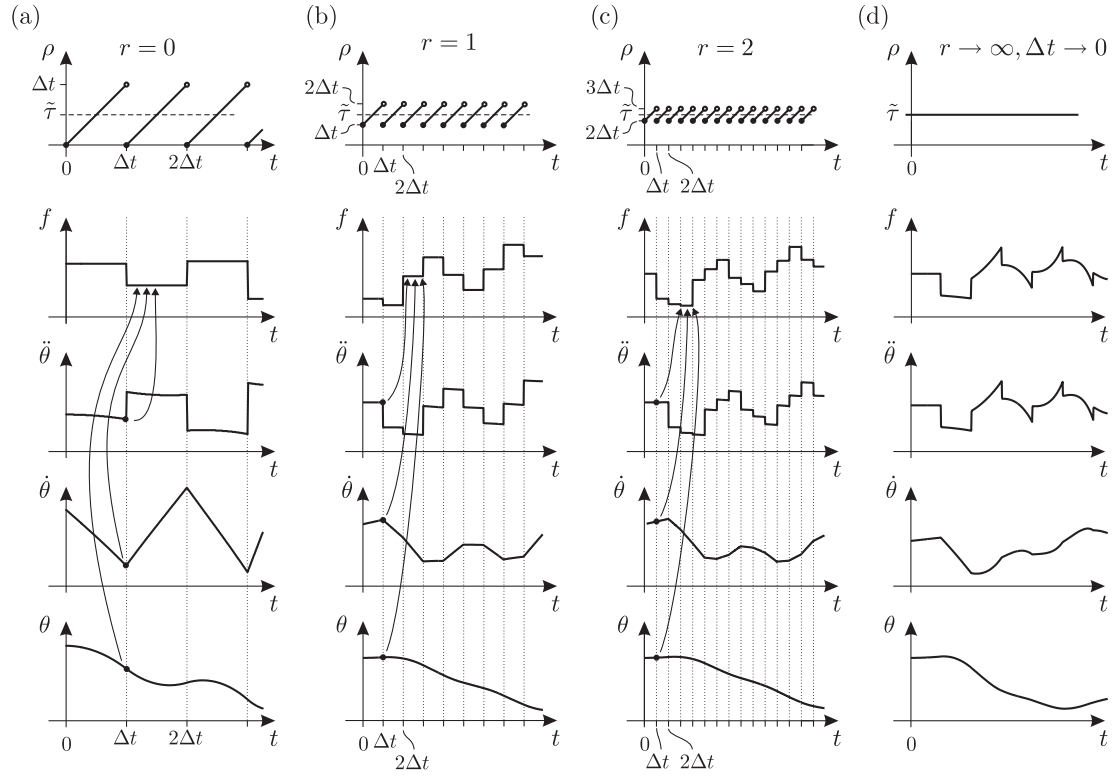

Fig. 2. Time-varying delay and sampling effect (a) for (2) (r=0); for (7) with (b) $r = 1$ and (c) $r = 2$; and (d) for (6).

decreasing the sampling period Δt such that the average delay remains constantly $\tilde{\tau} = \tau$. Clearly, if $r = 0$ then (7) is identical to (2). In the limit case, when $r \to \infty$ and $\Delta t \to 0$ such that $(r + 1/2)\Delta t = \tau$, the solution of (7) approaches that of (6). In this sense, the semi-discrete model (7) provides a transition between discrete-time and continuous-time representations of feedback control. Figure 2 shows the transition between the discrete-time model and the continuous-time model via the semi-discrete system (7). Note that the similar sawtooth-like delay was also used in stochastic delay models (Verriest and Michiels, 2009; Qin et al., 2014).

3. STABILIZABILITY CONDITIONS FOR THE DIFFERENT MODELS

It is known that feedback delay limits stabilizability of control systems. Here, the critical delay associated with the continuous-time model, the discrete-time model and the semi-discrete model is analyzed.

3.1 Discrete-time controller without feedback delay

Equation (2) can be written in the form

$$\dot{\mathbf{x}}(t) = \mathbf{A}\mathbf{x}(t) + \mathbf{B}(\mathbf{K}_{\rm pd}\mathbf{x}(t_i) + k_a\ddot{\theta}(t_i)) \,, \quad t \in [t_i, t_{i+1}) \tag{10}$$

where

$$\mathbf{x}(t) = \begin{pmatrix}\theta(t)\\ \dot{\theta}(t)\end{pmatrix}, \ \mathbf{A} = \begin{pmatrix}0 & 1\\ \omega_{\rm n}^2 & 0\end{pmatrix} \ \text{and} \ \mathbf{B} = \begin{pmatrix}0\\ -1\end{pmatrix} \tag{11}$$

and $\mathbf{K}_{\rm pd} = (k_{\rm p} \ k_{\rm d})$. Since the terms $\mathbf{x}(t_i)$ and $\ddot{\theta}(t_i))$ are piecewise constant over the sampling period, the solution at time instant t_{i+1} can be given using the variation of constants formula. This gives

$$\mathbf{x}(t_{i+1}) = \mathbf{A}_{\rm d}\mathbf{x}(t_i) + \mathbf{B}_{\rm d}(\mathbf{K}_{\rm pd}\mathbf{x}(t_i) - k_a\ddot{\theta}(t_i)), \tag{12}$$

$$\dot{\mathbf{x}}(t_{i+1}) = \mathbf{A}\mathbf{A}_{\rm d}\mathbf{x}(t_i) + (\mathbf{A}\mathbf{B}_{\rm d} + \mathbf{B})(\mathbf{K}_{\rm pd}\mathbf{x}(t_i) - k_a\ddot{\theta}(t_i)), \tag{13}$$

where

$$\mathbf{A}_{\rm d} = {\rm e}^{\mathbf{A}\Delta t}, \quad \mathbf{B}_{\rm d} = \int_0^{\Delta t} {\rm e}^{\mathbf{A}(\Delta t - s)}{\rm d}s\,\mathbf{B}. \tag{14}$$

Note that $\ddot{\theta}(t_{i+1}) = \mathbf{C}\dot{\mathbf{x}}(t_{i+1})$, where $\mathbf{C} = (0\ 1)$. Thus, a three-dimensional discrete map

$$\mathbf{z}_{i+1} = \mathbf{\Phi}\mathbf{z}_i \tag{15}$$

can be constructed, where $\mathbf{z}_i = \big(\theta(t_i)\ \dot{\theta}(t_i)\ \ddot{\theta}(t_i)\big)^{\rm T}$ and

$$\mathbf{\Phi} = \begin{pmatrix}\mathbf{A}_{\rm d} + \mathbf{B}_{\rm d}\mathbf{K}_{\rm pd} & k_{\rm a}\mathbf{B}_{\rm d}\\ \mathbf{C}(\mathbf{A}\mathbf{A}_{\rm d} + (\mathbf{A}\mathbf{B}_{\rm d} + \mathbf{B})\mathbf{K}_{\rm pd}) & k_{\rm a}\mathbf{C}(\mathbf{A}\mathbf{B}_{\rm d} + \mathbf{B})\end{pmatrix}. \tag{16}$$

If matrices $\mathbf{A}$, $\mathbf{B}$, $\mathbf{C}$ and $\mathbf{K}_{\rm pd}$ are substituted, then one obtains

$$\mathbf{\Phi} = \begin{pmatrix}\frac{k_{\rm p}(1-{\rm ch})+\omega_{\rm n}^2{\rm ch}}{\omega_{\rm n}^2} & \frac{k_{\rm d}(1-{\rm ch})+\omega_{\rm n}{\rm sh}}{\omega_{\rm n}^2} & \frac{k_{\rm a}({\rm ch}-1)}{\omega_{\rm n}^2}\\ \frac{(\omega_{\rm n}^2-k_{\rm p}){\rm sh}}{\omega_{\rm n}} & \frac{\omega_{\rm n}{\rm ch}-k_{\rm d}{\rm sh}}{\omega_{\rm n}} & \frac{k_{\rm a}{\rm sh}}{\omega_{\rm n}}\\ (\omega_{\rm n}^2 - k_{\rm p}){\rm ch} & \omega_{\rm n}{\rm sh} - k_{\rm d}{\rm ch} & k_{\rm a}{\rm ch}\end{pmatrix}, \tag{17}$$

where ${\rm sh} = \sinh(\omega_{\rm n}\Delta{\rm t})$ and ${\rm ch} = \cosh(\omega_{\rm n}\Delta{\rm t})$. Stability properties are determined by the eigenvalues of matrix $\mathbf{\Phi}$. If all the eigenvalues are in modulus less than one, then the system is asymptotically stable.

The D-curves can be analyzed by the substitution of $z = 1$, $z = -1$ and $z = {\rm e}^{{\rm i}\omega}$ ($\omega \in [0, \pi]$) into the characteristic equation $\det(\mathbf{\Phi} - z\mathbf{I}) = 0$. It can be shown that the system is asymptotically stable if

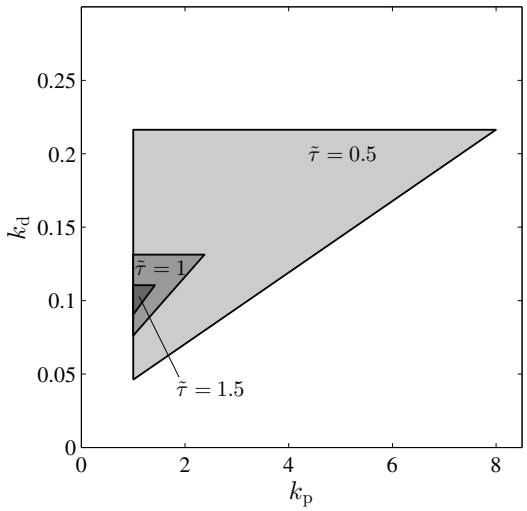

Fig. 3. Stability diagram for (2) with $\omega_\mathrm{n}^2 = 1$, $k_\mathrm{a} = 0.9$ for different average delays $\tilde{\tau}$.

$$|k_\mathrm{a}| < 1 \tag{18}$$

$$\text{and} \quad k_\mathrm{p} > \omega_\mathrm{n}^2 \tag{19}$$

$$\text{and} \quad k_\mathrm{d} < \frac{\omega_\mathrm{n}(1-k_\mathrm{a})(\mathrm{e}^{\omega_\mathrm{n}\Delta t}+1)}{(\mathrm{e}^{\omega_\mathrm{n}\Delta t}-1)} \tag{20}$$

$$\text{and} \quad k_\mathrm{d} > \frac{(\mathrm{e}^{\omega_\mathrm{n}\Delta t}-1)(1-k_\mathrm{a})\Big(k_\mathrm{p}+\omega_\mathrm{n}^2 k_\mathrm{a}\Big)}{\omega_\mathrm{n}(\mathrm{e}^{\omega_\mathrm{n}\Delta t}+1)(k_\mathrm{a}+1)}. \tag{21}$$

A sample stability diagram is shown in Figure 3 for different average delays (note that $\tilde{\tau} = \Delta t/2$). It can be observed that the stable domain shrinks as the delay is increased. However, the stable region does not disappear as $\Delta t \to \infty$. This means that, in theory, the system can be stabilized for any large sampling period Δt (i.e., for any average delay $\tilde{\tau}$).

3.2 Continuous-time controller with feedback delay

Stability analysis of (6) was performed by Sieber and Krauskopf (2005) and later by Insperger et al. (2013) in context of human balancing. It is known that if $|k_\mathrm{a}| > 1$, then (6) is unstable with infinitely many characteristic roots with positive real parts (see Lemma 3.9 on page 63 in Stepan (1989)), therefore, a necessary criteria for the stability of (6) is that $|k_\mathrm{a}| < 1$. The characteristic equation reads

$$(1 + k_\mathrm{a}\mathrm{e}^{-\tau s})s^2 + k_\mathrm{d}\mathrm{e}^{-\tau s}s - \omega_\mathrm{n}^2 + k_\mathrm{p}\mathrm{e}^{-\tau s} = 0. \tag{22}$$

Substitution of $s = \mathrm{e}^{\mathrm{i}\omega}$ and decomposition into real and imaginary parts give the D-curves in the form

$$\text{if } \omega = 0: \quad k_\mathrm{p} = \omega_\mathrm{n}^2, \quad k_\mathrm{d} \in \mathbb{R}, \tag{23}$$

$$\text{if } \omega \neq 0: \quad \begin{cases} k_\mathrm{p} = (\omega^2 + \omega_\mathrm{n}^2)\cos(\omega\tau) + k_\mathrm{a}\omega^2, \\ k_\mathrm{d} = \frac{\omega^2+\omega_\mathrm{n}^2}{\omega}\sin(\omega\tau). \end{cases} \tag{24}$$

Here, $\omega \in [0, \infty)$ is the frequency parameter. The D-curves separate the plane $(k_\mathrm{p}, k_\mathrm{d})$ into domains where the numbers of unstable characteristic exponents are constant. The stability boundaries are the D-curves bounding the domains with zero unstable characteristic exponent.

Stability diagram of (6) for different delays is shown in Figure 4. Stable regions are indicated by gray shading of different intensity associated with different delays. It can

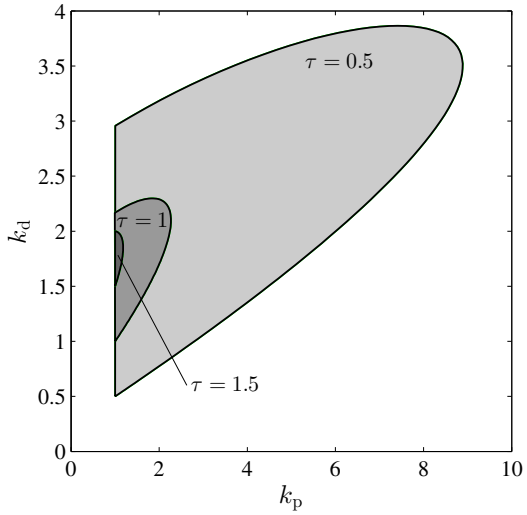

Fig. 4. Stability diagram for (6) with $\omega_\mathrm{n}^2 = 1$, $k_\mathrm{a} = 0.9$ for different delays τ.

be observed that the stable domain shrinks as the delay is increased. As shown by Sieber and Krauskopf (2005) and Insperger et al. (2013), the stable domain disappears at a critical delay value. This happens if the slope of the D-curves (24) at $\omega = 0$ becomes vertical. The critical delay, which limits stabilizability, is

$$\tau_\mathrm{crit,cont} = \frac{\sqrt{2k_\mathrm{a}+2}}{\omega_\mathrm{n}}, \tag{25}$$

which, at the limit case $k_\mathrm{a} = 1$ gives

$$\tau_\mathrm{crit,cont} = \frac{2}{\omega_\mathrm{n}}. \tag{26}$$

If the feedback delay is larger than $\tau_\mathrm{crit,cont}$, then the system is unstable for any k_p, k_d and $|k_\mathrm{a}| < 1$.

3.3 Semi-discretization of time-delayed feedback

Equation (7) can be written in the form

$$\dot{\mathbf{x}}(t) = \mathbf{A}\mathbf{x}(t) + \mathbf{B}\, v_{i-r} \quad t \in [t_i, t_{i+1}) \tag{27}$$

$$v_{i-r} = \mathbf{K}_\mathrm{pd}\mathbf{x}(t_{i-r}) + k_a\ddot{\theta}(t_{i-r}), \tag{28}$$

where $\mathbf{x}(t)$, $\mathbf{A}$, $\mathbf{B}$ and $\mathbf{K}_\mathrm{pd}$ are defined in (11). Similarly to the discrete-time case, the solution at time instant t_{i+1} can be given as

$$\mathbf{x}(t_{i+1}) = \mathbf{A}_\mathrm{d}\mathbf{x}(t_i) + \mathbf{B}_\mathrm{d}\, v_{i-r}, \tag{29}$$

$$\dot{\mathbf{x}}(t_{i+1}) = \mathbf{A}\mathbf{A}_\mathrm{d}\mathbf{x}(t_i) + (\mathbf{A}\mathbf{B}_\mathrm{d} + \mathbf{B})\, v_{i-r}, \tag{30}$$

where $\mathbf{A}_\mathrm{d}$ and $\mathbf{B}_\mathrm{d}$ are given in (14). Note that here $\Delta t = \tilde{\tau}/(r + 1/2)$.

Equations (28), (29) and (30) imply the $(r+3)$-dimensional discrete map

$$\mathbf{z}_{i+1} = \mathbf{\Phi}\mathbf{z}_i, \tag{31}$$

where

$$\mathbf{z}_i = \begin{pmatrix} \theta(t_i) \\ \dot{\theta}(t_i) \\ \ddot{\theta}(t_i) \\ v_{i-1} \\ v_{i-2} \\ \vdots \\ v_{i-r} \end{pmatrix}, \quad \mathbf{\Phi} = \begin{pmatrix} \mathbf{A}_\mathrm{d} & \mathbf{0} & 0 & \cdots & 0 & \mathbf{B}_\mathrm{d} \\ \mathbf{C}\mathbf{A}\mathbf{A}_\mathrm{d} & 0 & 0 & \cdots & 0 & \mathbf{R}_\mathrm{d} \\ \mathbf{K}_\mathrm{pd} & k_\mathrm{a} & 0 & \cdots & 0 & 0 \\ \mathbf{0} & 0 & 1 & \cdots & 0 & 0 \\ \vdots & & & & & \vdots \\ \mathbf{0} & 0 & 0 & \cdots & 0 & 0 \\ \mathbf{0} & 0 & 0 & \cdots & 1 & 0 \end{pmatrix} \tag{32}$$

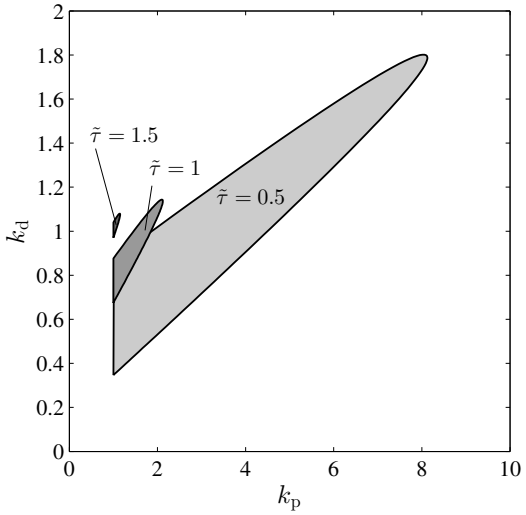

Fig. 5. Stability diagram for (7) with $r = 1$, $\omega_\mathrm{n}^2 = 1$, $k_\mathrm{a} = 0.9$ for different average delays $\tilde{\tau}$.

with $\mathbf{R}_\mathrm{d} = \mathbf{C}(\mathbf{A}\mathbf{B}_\mathrm{d}+\mathbf{B})$ and $\mathbf{C} = (0\ 1)$. After substitution of the matrices $\mathbf{A}$, $\mathbf{B}$, $\mathbf{C}$ and $\mathbf{K}_\mathrm{pd}$ one obtains

$$\mathbf{\Phi} = \begin{pmatrix} \mathrm{ch} & \frac{\mathrm{sh}}{\omega_\mathrm{n}} & 0 & 0 \dots 0 & \frac{1-\mathrm{ch}}{\omega_\mathrm{n}^2} \\ \omega_\mathrm{n}\mathrm{sh} & \mathrm{ch} & 0 & 0 \dots 0 & -\frac{\mathrm{sh}}{\omega_\mathrm{n}} \\ \omega_\mathrm{n}^2\mathrm{ch} & \omega_\mathrm{n}\mathrm{sh} & 0 & 0 \dots 0 & -\mathrm{ch} \\ k_\mathrm{p} & k_\mathrm{d} & k_\mathrm{a} & 0 \dots 0 & 0 \\ 0 & 0 & 0 & 1 \dots 0 & 0 \\ \vdots & & & \ddots & \vdots \\ 0 & 0 & 0 & 0 \dots 1 & 0 \end{pmatrix}, \tag{33}$$

where $\mathrm{sh} = \sinh(\omega_\mathrm{n}\Delta\mathrm{t})$ and $\mathrm{ch} = \cosh(\omega_\mathrm{n}\Delta\mathrm{t})$. Stability properties are determined by the eigenvalues of matrix $\mathbf{\Phi}$.

Again, the D-curves can be analyzed by the substitution of $z = 1$, $z = -1$ and $z = \mathrm{e}^{\mathrm{i}\omega}$ ($\omega \in [0, \pi]$) into the characteristic equation $\det(\mathbf{\Phi} - z\mathbf{I}) = 0$. For instance, for the case $r = 1$, the D-curves read

$$\text{if } z = 1: \qquad k_\mathrm{p} = \omega_\mathrm{n}^2, \quad k_\mathrm{d} \in \mathbb{R}, \tag{34}$$

$$\text{if } z = -1: \quad k_\mathrm{d} = -\frac{\omega_\mathrm{n}(k_\mathrm{a}+1)(\mathrm{e}^{\omega_\mathrm{n}\Delta t}+1)}{\mathrm{e}^{\omega_\mathrm{n}\Delta t}-1}, \quad k_\mathrm{p} \in \mathbb{R}, \tag{35}$$

if $z = \mathrm{e}^{\mathrm{i}\omega}$, $\omega \in (0, \pi)$:

$$\begin{aligned} k_\mathrm{p} = &-\frac{\omega_\mathrm{n}^2}{(\mathrm{e}^{\omega_\mathrm{n}\Delta t}-1)^2}\Big(4\mathrm{e}^{\omega_\mathrm{n}\Delta t}\cos^2\omega \\ &- 2(\mathrm{e}^{2\omega_\mathrm{n}\Delta t}+\mathrm{e}^{\omega_\mathrm{n}\Delta t}+1+k_\mathrm{a}\mathrm{e}^{\omega_\mathrm{n}\Delta t})\cos\omega \\ &+ \mathrm{e}^{2\omega_\mathrm{n}\Delta t} - 2k_\mathrm{a}\mathrm{e}^{\omega_\mathrm{n}\Delta t}+1\Big), \end{aligned} \tag{36}$$

$$\begin{aligned} k_\mathrm{d} = &\frac{\omega_\mathrm{n}}{\mathrm{e}^{2\omega_\mathrm{n}\Delta t}-1}\Big(2\cos\omega - k_\mathrm{a}+1\Big) \\ &\times\Big(\mathrm{e}^{2\omega_\mathrm{n}\Delta t} - 2\mathrm{e}^{\omega_\mathrm{n}\Delta t}\cos\omega+1\Big). \end{aligned} \tag{37}$$

The corresponding stability diagram is shown in Figure 5 for different average delays. Similarly to the previous cases, the stable domain shrinks as the average delay is increased.

If $r = 1$ then the stable region disappears when the slope of the D-curves (36)-(37) at $\omega = 0$ becomes vertical. After some algebraic manipulation, the critical sampling period can be obtained as

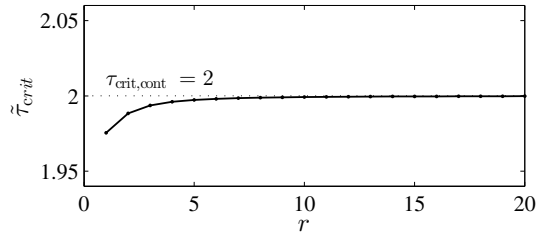

Fig. 6. Critical average delay for (7) with $\omega_\mathrm{n}^2 = 1$, $k_\mathrm{a} = 1$ for different r.

$$\Delta t_{\mathrm{crit},1} = \frac{1}{\omega_\mathrm{n}}\ln\left(\frac{3}{2}+\frac{1}{2}k_\mathrm{a}+\frac{1}{2}\sqrt{5+6k_\mathrm{a}+k_\mathrm{a}^2}\right). \tag{38}$$

If we set $k_\mathrm{a} = 0$ then we get the well-known critical sampling period for the discrete-time PD controller (Enikov and Stepan, 1998). The critical value for the average delay is

$$\tilde{\tau}_{\mathrm{crit},1} = \frac{3}{2\omega_\mathrm{n}}\ln\left(\frac{3}{2}+\frac{1}{2}k_\mathrm{a}+\frac{1}{2}\sqrt{5+6k_\mathrm{a}+k_\mathrm{a}^2}\right). \tag{39}$$

For the general case $r \geq 1$ (with $(r+\frac{1}{2})\Delta t = \tilde{\tau}$), the critical sampling period associated with a vertical slope of the D-curve at $\omega = 0$ can be given as

$$\Delta t_{\mathrm{crit},r} = \frac{1}{\omega_\mathrm{n}}\ln\left(\frac{r(r+1)+1+k_\mathrm{a}+\sqrt{(k_\mathrm{a}+2r(r+1)+1)(k_\mathrm{a}+1)}}{r(r+1)}\right). \tag{40}$$

If $k_\mathrm{a} = 0$ then this formula gives the critical sampling period for the semi-discrete PD controller (Insperger and Stepan, 2007; Insperger and Milton, 2014). The critical value for the average delay is

$$\tilde{\tau}_{\mathrm{crit},r} = \frac{r+\frac{1}{2}}{\omega_\mathrm{n}}\ln\left(\frac{r(r+1)+1+k_\mathrm{a}+\sqrt{(k_\mathrm{a}+2r(r+1)+1)(k_\mathrm{a}+1)}}{r(r+1)}\right). \tag{41}$$

In order to make the transition between the semi-discrete system (7) and the continuous-time system (6), the limit $\Delta t \to 0$, $r \to \infty$ with $\Delta t(r+\frac{1}{2}) = \tilde{\tau} = \tau$ should be investigated. Using (41), this limit gives

$$\lim_{\Delta t\to 0, r\to\infty}\tilde{\tau}_{\mathrm{crit},r} = \frac{\sqrt{2k_\mathrm{a}+2}}{\omega_\mathrm{n}}, \tag{42}$$

which is just equal to the critical delay $\tau_{\mathrm{crit,cont}}$ for the continuous-time delayed feedback control.

Figure 6 shows the variation of the critical average delay for different r. The convergence to the critical delay of the continuous-time delayed feedback control can be clearly observed. The difference between the critical delay $\tilde{\tau}_{\mathrm{crit},1}$ for the semi-discrete system with $r = 1$ and the critical delay $\tau_{\mathrm{crit,cont}}$ for the continuous-time delayed feedback control is about 1.2%. If $r = 2$, then the difference is 0.6%. Although there are several differences between the continuous-time, the discrete-time and the semi-discrete models, these observation implies that, from the point of stabilizability, the different models give about the same critical delay.

4. CONCLUSION

The transition between continuous-time and discrete-time delayed PDA controllers was established by means of the semi-discretization method. The critical delay, which limits stabilizability of the system, was determined for

each model. It was shown that although the different models uses fundamentally different timing concept for the feedback, they all provide about the same critical value for the average delay.

Note that in this analysis only the slopes of the D-curves were analyzed, but stabilizability in discrete cases can also be affected by the D-curve associated with $z = -1$. This case, however, show up only in the cases when $1 < r < \infty$. For the cases $r = 1$ and $r \to \infty$ (continuous-time model), the sufficient condition for the loss of stabilizability is the vertical slope of the D-curves at $\omega = 0$ if $|k_a| < 1$.

Note furthermore that adding an integral term to the controller does not extend the limit of stabilizability, since in case of the critical delay, the integral control gain is 0 (Lehotzky and Insperger, 2014).

ACKNOWLEDGEMENTS

This work was supported by the Hungarian National Science Foundation under grant OTKA-K105433 and by the William R Kenan Jr Charitable Trust (JM).

REFERENCES

Asai, Y., Tanaka, Y., Nomura, K., Nomura, T., Casidio, M., and Morasso, P. (2009). A model of postural control in quiet standing: Robust compensation of delay-induced instability using intermittent activation of feedback control. *PLoS ONE*, 4. E6169.

Burdet, E. and Milner, T.E. (1998). Quantization of human motions and learning of accurate movements. *Biol Cybern*, 78, 307–318.

Cabrera, J.L. and Milton, J.G. (2002). On-off intermittency in a human balancing task. *Phys. Rev. Lett.*, 89. 158702.

Cluff, T. and Balasubramaniam, R. (2009). Motor learning characterized by changing Lévy distributions. *PLoS ONE*, 4, e5998.

Enikov, E. and Stepan, G. (1998). Micro-chaotic motion of digitally controlled machines. *J Vib Control*, 2, 427–443.

Foo, P., Kelso, J.A.S., and de Guzman, G.C. (2000). Functional stabilization of fixed points: Human pole balancing using time to balance information. *J Exp Psychol Human Percept Perform*, 26, 1281–1292.

Gawthrop, P., Gollee, H., Mamma, A., Loram, I., and Lakie, M. (2013). Human stick balancing: an intermittent control explanation. *Biol Cybern*, 107, 637–652.

Insperger, T. and Milton, J. (2014). Sensory uncertainty and stick balancing at the fingertip. *Biol Cybern*, 108. 85-101.

Insperger, T., Milton, J., and Stepan, G. (2013). Acceleration feedback improves balancing against reflex delay. *J R Soc Interface*, 10(79). 20120763.

Insperger, T. and Stepan, G. (2007). Act-and-wait control concept for discrete-time systems with feedback delay. *IET Control Theory A*, 1(3). 553-557.

Insperger, T. and Stepan, G. (2011). *Semi-Discretization for Time-Delay Systems*. Springer, New York.

Insperger, T., Stepan, G., and Turi, J. (2010). Delayed feedback of sampled higher derivatives. *Phil Trans Roy Soc A*, 368(1911). 469-482.

Jirsa, V.K., Fink, P., Foo, P., and Kelso, J.A.S. (2000). Parametric stabilization of biological coordination: a theoretical model. *J Biol Phys*, 26, 85–112.

Lee, K.Y., O'Dwyer, N., Halaki, M., and Smith, R. (2012). A new paradigm for human stick balancing: a suspended not an inverted pendulum. *Exp Brain Res*, 221, 309–328.

Lehotzky, D. and Insperger, T. (2014). The mechanical modeling of human balancing using PIDA control (in Hungarian). *Biomechanica Hungarica*, VII, 24.33.

Lockhart, D.B. and Ting, L.H. (2007). Optimal sensorimotor transformations for balance. *Nature Neurosci.*, 10, 1329–1336.

Loram, I.D., Gollee, H., Lakie, M., and Gawthrop, P.J. (2011). Human control of an inverted pendulum: Is continuous control necessary? is intermittent control effective? is intermittent control physiological? *J Physiol*, 589, 307–324.

Loram, I.D., van de Kamp, C., M. Lakie, a.H.G., and Gawthrop, P.J. (2014). Does the motor system need intermittent control? *Exer Sport Sci*, 42. 117-25.

Miall, R.C., Weir, D.J., and Stein, R.F. (1993). Intermittency in human manual tracking tasks. *J Mot Behav*, 25, 53–63.

Michiels, W. and Niculescu, S.I. (2007). *Stability and stabilization of time-delay systems: an eigenvalue-based approach*. SIAM Publications, Philadelphia.

Milton, J., Cabrera, J.L., Ohira, T., Tajima, S., Tonoskai, Y., Eurich, C.W., and Campbell, S.A. (2009a). The time-delayed, inverted pendulum: Implications for human balance control. *Chaos*, 19. 026110.

Milton, J.G., Ohira, T., Cabrera, J.L., Fraiser, R.M., Gyorffy, J.B., Ruiz, F.K., Strauss, M.A., Balch, E.C., Marin, P.J., and Alexander, J.L. (2009b). Balancing with vibration: A prelude for "drift and act" balance control. *PLoS ONE*, 4, e7427.

Nataraj, R., Audu, M.L., Kirsch, R.F., and Triolo, R.J. (2012). Center of mass acceleration feedback control for standing by functional neuromuscular stimulation: a stimulation study. *J Rehabil Res Dev*, 49, 279–296.

Peterka, R.J., III, C.W., and Kentala, E. (2006). Determining the effectiveness of a vibrotactile balance prothesis. *J Vest Res*, 16, 45–56.

Qin, W.B., Gomez, M.M., and Orosz, G. (2014). Stability analysis of connected cruise control with stochastic delays. In *Proceedings of the American Control Conference, IEEE*, 4624–4629.

Sieber, J. and Krauskopf, B. (2005). Extending the permissible control loop latency for the controlled inverted pendulum. *Dynam Syst*, 20(2), 189–199.

Stepan, G. (1989). *Retarded dynamical systems*. Longman, Harlow.

Stepan, G. (2009). Delay effects in the human sensory system during balancing. *Philos T Roy Soc A*, 367, 1195–1212.

van de Kamp, C., Gawthrop, P.J., Gollee, H., and Loram, I.D. (2013). Refractoriess in sustained visuo-manual control: Is the refractory duration intrinsic or does it depend on external system properties? *PLoS Comp Biol*, 9. E1002843.

Verriest, E.I. and Michiels, W. (2009). Stability analysis of systems with stochastically varying delays. *Syst Control Lett*, 58, 783–791.

Welch, T.D.J. and Ting, L.H. (2008). A feedback model reproduces muscle activity during human postural responses to support-surface translations. *J Neurophysiol*, 99, 1032–1038.